

Supporting Information

A Near-Infrared Water-Soluble Fluorescent Probe for the Detection of Biothiols in Living Cells and Escherichia Coli

Ling-Ling Li, Pei-Yang He, Sheng-Lin Pan, Lei Shi, Meng-Yang Li, Qian Zhou, Hong Zhang, Nan Wang, Kun Li*, Xiao-Qi Yu*

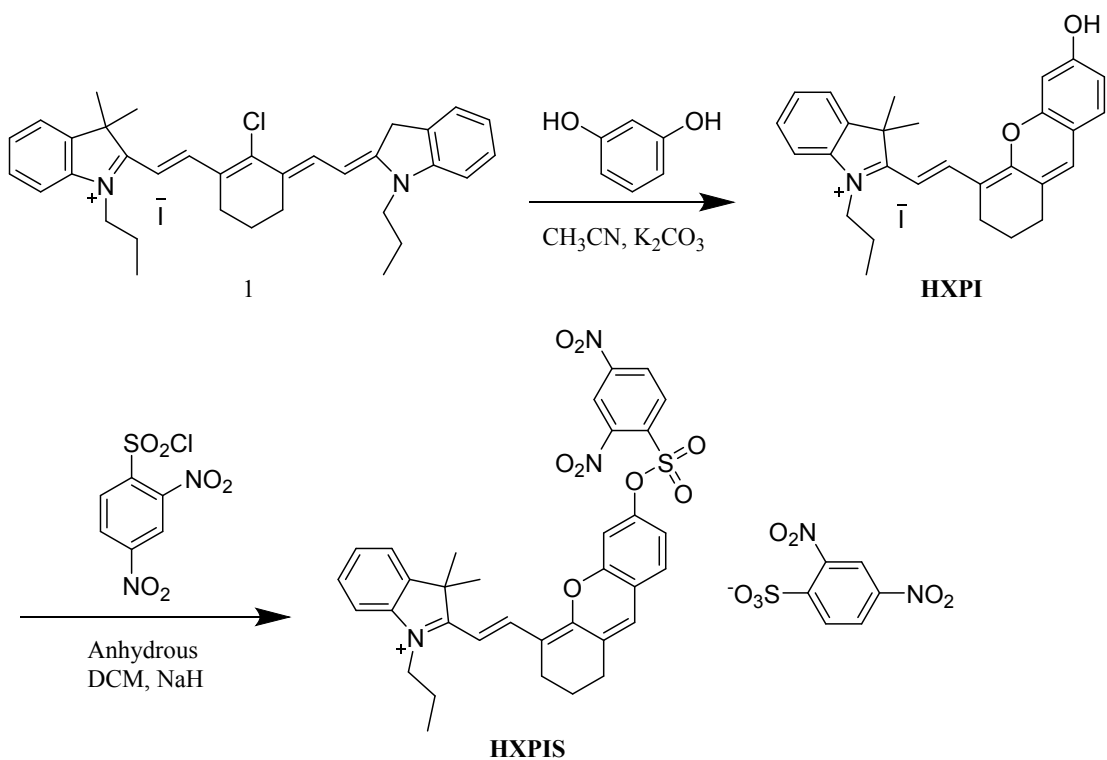
Key Laboratory of Green Chemistry and Technology, Ministry of Education, College of Chemistry, Sichuan University, No. 29, Wangjiang Road, Chengdu, 610064, P.R. China.

**Correspondence and requests for materials should be addressed to Kun- Li (kli@scu.edu.cn) or Xiao-Qi Yu (xqyu@scu.edu.cn)*

Contents

1. Synthesis of Compounds	S2
2. Molar Extinction Coefficient	S3
3. UV spectra	S3
4. Time-dependent fluorescence changes of HXPIS with biothiols	S4
5. Fluorometric titration experiment	S5
6. Limit of detection	S5
7. pH influence	S7
8. Selectivity of the probe HXPIS towards biothiols	S7
9. Determination of the cleavage product through $^1\text{H-NMR}$ and HRMS tests	S9
10. Cytotoxicity experiments	S9
11. Table S1. Summary of the optical properties of representative near infrared fluorescent probes for distinguishing biothiols.	S9
12. NMR and HRMS spectra of HXPIS	S13

1. Synthesis of Compounds



Scheme S1. Synthetic route of HXPIS.

Compound 1 and HXPI were prepared referring to the literature reports.¹⁻²

HXPIS: To a solution of HXPI (500.0 mg, 0.93 mmol) in dry CH_2Cl_2 (10 mL), NaH (110 mg, 2.79 mmol) was added. The mixture was stirred at room temperature for 30 min. Then 2,4-dinitrobenzenesulfonyl chloride (740 mg, 2.79 mmol) was diluted in 10 mL CH_2Cl_2 and added dropwise to the solution. The mixture was stirred at room temperature for another 5 hours. The color of the reaction changed from deep blue to purple. The solvent was removed under reduced pressure and the crude product was purified by column chromatography over silica gel eluting with $\text{CH}_2\text{Cl}_2/\text{CH}_3\text{OH} = 80:1$ to afford purple solid (463 mg, yield 56.0%). $^1\text{H-NMR}$ (400 MHz, DMSO-d_6) δ 0.93–0.97 (t, $J_1=8.0$ Hz, $J_2=8.0$ Hz, 3H), 1.71(s, 6H), 1.79 – 1.85 (m, 4H), 2.64–2.67 (m, 4H), 4.43–4.46 (t, $J_1=8.0$ Hz, $J_2=4.0$ Hz, 2H), 6.69–6.73 (d, $J=16.0$, 1H), 6.99–7.02 (d, $J=12.0$ Hz, 1H), 7.30 (s, 1H), 7.50–7.57 (m, 3H), 7.42 (s, 1H), 7.76–7.79 (t, $J_1=4.0$ Hz, $J_2=8.0$ Hz, 2H), 8.04–8.06 (d, $J=8.0$ Hz, 1H), 8.33–8.37 (m, 2H), 8.48–8.51 (m, 2H), 8.60–8.63 (d, $J = 8.0$ Hz, 1H), δ 9.14 (s, 1H). $^{13}\text{C-NMR}$ (101 MHz, DMSO-d_6) δ 11.4, 20.1, 21.7, 23.9, 27.5, 29.1, 47.1, 51.5, 107.8, 110.6, 114.6, 115.1, 118.7, 121.6, 121.9, 123.2, 126.1, 128.0, 128.5, 129.4, 129.5, 131.1, 131.2, 131.5, 134.2, 141.7, 143.1, 145.1, 145.9, 147.8, 148.6, 149.6, 152.0, 152.9, 158.2, 174.3, 179.7. HRMS (ESI) m/z calcd. for $\text{C}_{34}\text{H}_{32}\text{N}_3\text{O}_8\text{S}^+$ (M^+): 642.1905. Found: 642.1903.

2. Molar Extinction Coefficient

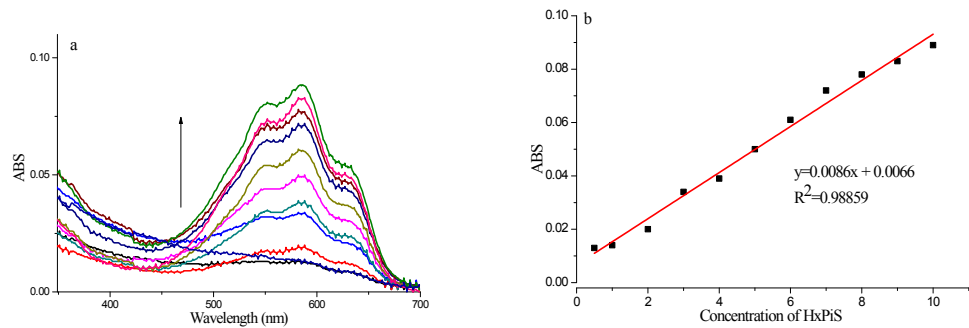


Figure S1. (a) UV spectra of HXPIS at different concentrations (0.5, 1, 2, 3, 4, 5, 6, 7, 8, 9, 10 μM) (b) Absorption-concentration curve of HXPIS.

3. UV spectra

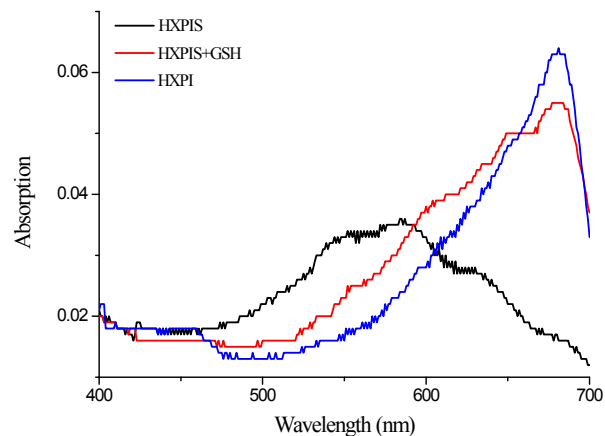


Figure S2. Absorption spectra of HXPIS (5 μM), HXPIS (5 μM) with GSH (100 μM), and HXPI (5 μM) in PBS buffer solution (10 mM, pH 7.4).

4. Time-dependent fluorescence changes of HXPIS with biothiols.

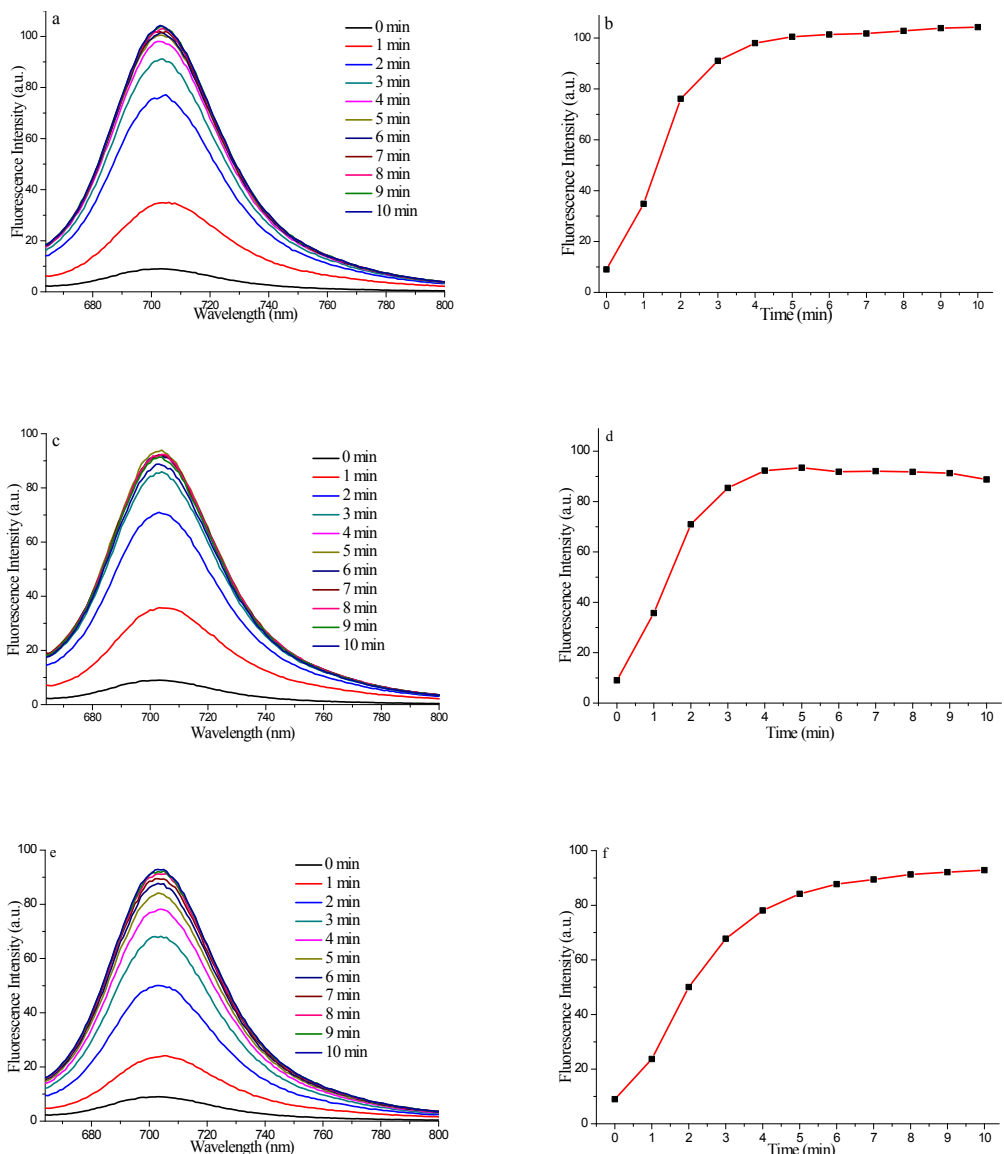


Figure S3. Time-dependent fluorescence changes of HXPIS (5 μ M) to (a) GSH, (b) Cys and (c) Hcy; Fluorescence intensity changes at 703 nm of HXPIS with (d) GSH, (e) Cys and (f) Hcy at different indicated time.

5. Fluorometric titration experiment

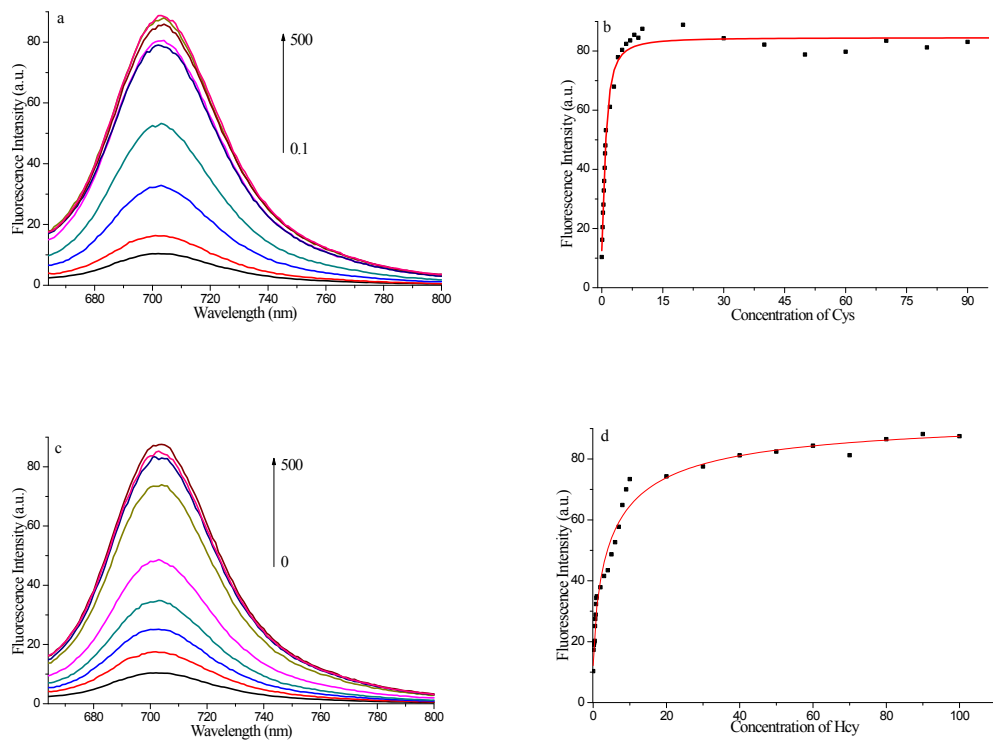


Figure S4. Fluorescence changes of HXPIS (5 μM) on the incremental addition of (a) Cys, (c) Hey; The tendency chart of the fluorescence intensity of HXPIS with the increased concentration of (b) Cys, (d) Hey.

6. Limit of detection

The limit of detection, expressed as the concentration, CL , $CL = 3\sigma/m$

$$\sigma = \sqrt{\frac{\sum(x - x_i)^2}{n - 1}}$$

x is the mean of the blank measures (probe only), x_i is the values of blank measures, n is the tested number of blank measures, m is the slope of the linear regression equation.

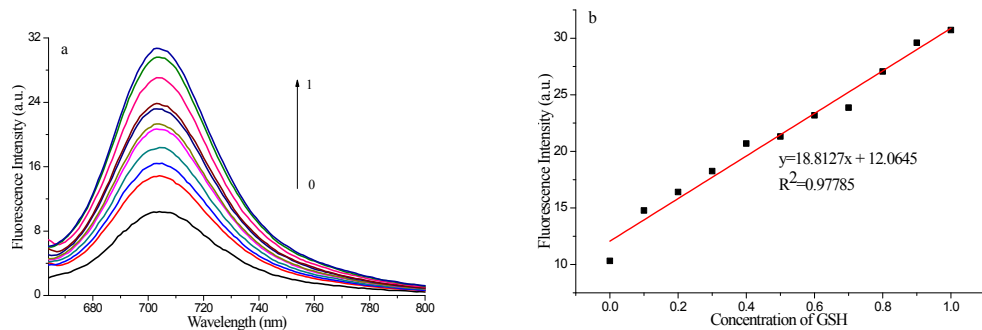


Figure S5. (a) The fluorescence response of the probe HXPIS to GSH at the varied concentrations (0-1 μM). (b) A linear correlation between fluorescent response and concentration of GSH. The

spectra were recorded in PBS buffer (pH 7.4, 10 mM). $\lambda_{\text{ex/em}} = 654/703$ nm.

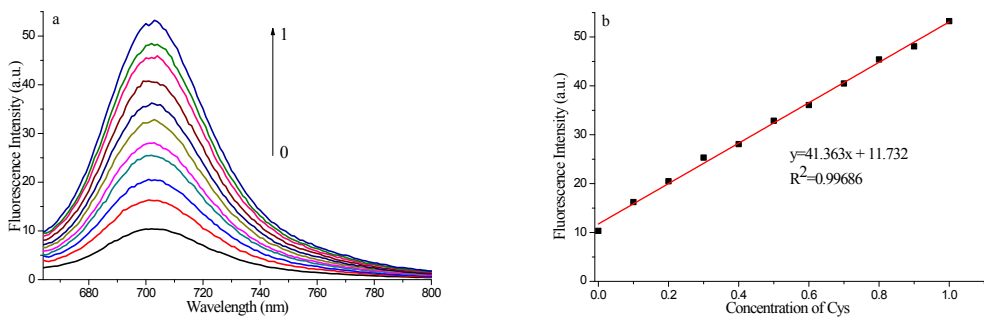


Figure S6. (a) The fluorescence response of the probe HXPIS to Cys at the varied concentrations (0-1 μ M). (b) A linear correlation between fluorescent response and concentration of Cys. The spectra were recorded in PBS buffer (pH 7.4, 10 mM). $\lambda_{\text{ex/em}} = 654/703$ nm.

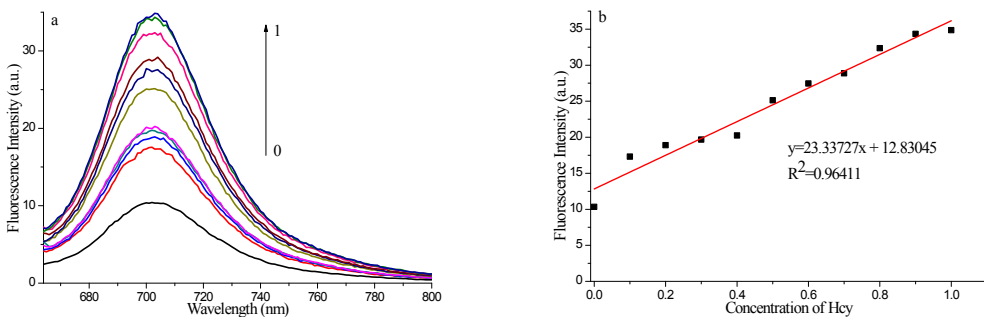


Figure S7. (a) The fluorescence response of the probe HXPIS to Hcy at the varied concentrations (0-1 μ M). (b) A linear correlation between fluorescent response and concentration of Hcy. The spectra were recorded in PBS buffer (pH 7.4, 10 mM). $\lambda_{\text{ex/em}} = 654/703$ nm.

7. pH influence

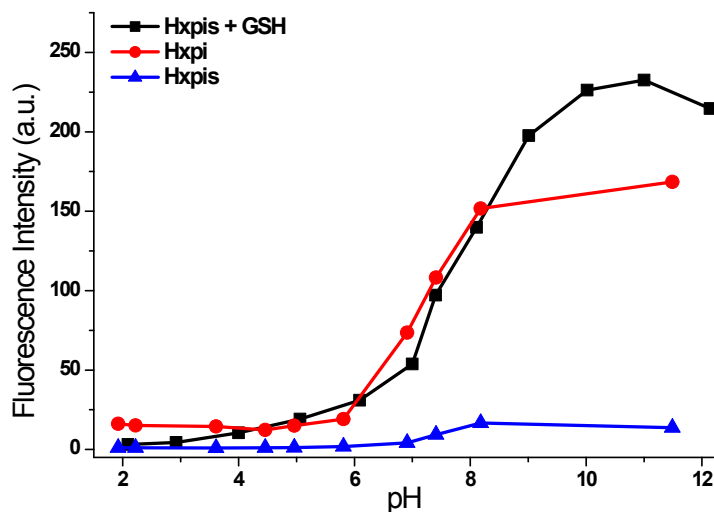
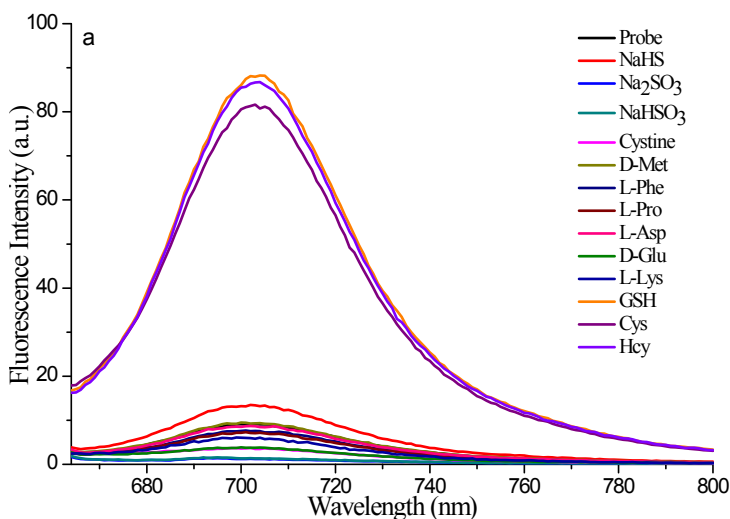


Figure S8. Effects of pH on the fluorescence of HXPIS (5 μ M) + GSH (100 μ M), HXPI (5 μ M) and HXPIS (5 μ M). Conditions: 10 mM PBS, pH 7.4. $\lambda_{\text{ex}}/\lambda_{\text{em}} = 654 / 703$ nm.

8. Selectivity of the probe HXPIS towards biothiols.



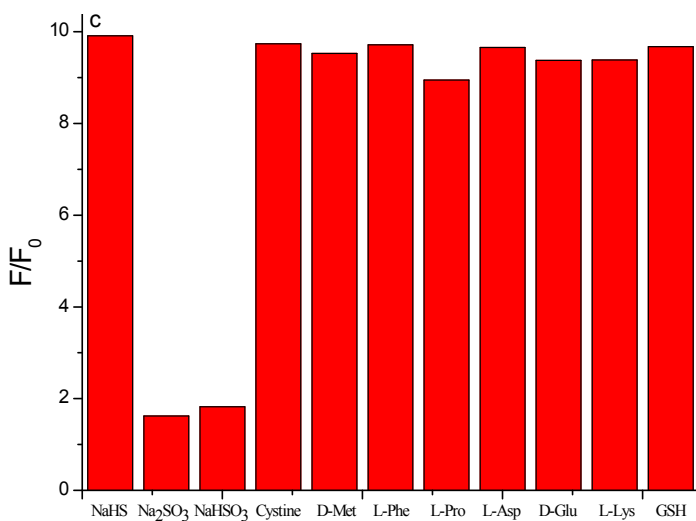
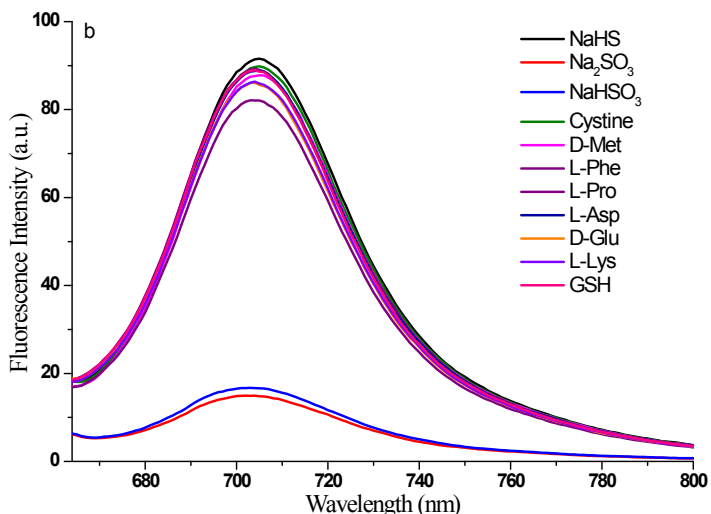


Figure S9. (a) The fluorescence spectra of the probe HXPIS ($5 \mu\text{M}$) in the presence of various relevant analytes (20 equiv. of NaHS, Na_2SO_3 , NaHSO_3 , Cystine, D-Met, L-Phe, L-Pro, L-Asp, D-Glu, L-Lys, Cys, Hcy and GSH). (b) The fluorescence spectra of HxpiS ($5 \mu\text{M}$) upon the addition of different interferents (NaHS, Na_2SO_3 , NaHSO_3 , Cystine, D-Met, L-Phe, L-Pro, L-Asp, D-Glu, L-Lys, $100 \mu\text{M}$) in the presence of GSH ($100 \mu\text{M}$) in PBS (pH = 7.4, $\lambda_{\text{ex}}/\lambda_{\text{em}} = 654 / 703 \text{ nm}$). (c) The histogram of (b). The data were obtained after the incubation of the probe HXPIS with the analytes at 37°C for 30 min.

9. Determination of the cleavage product through HRMS test.

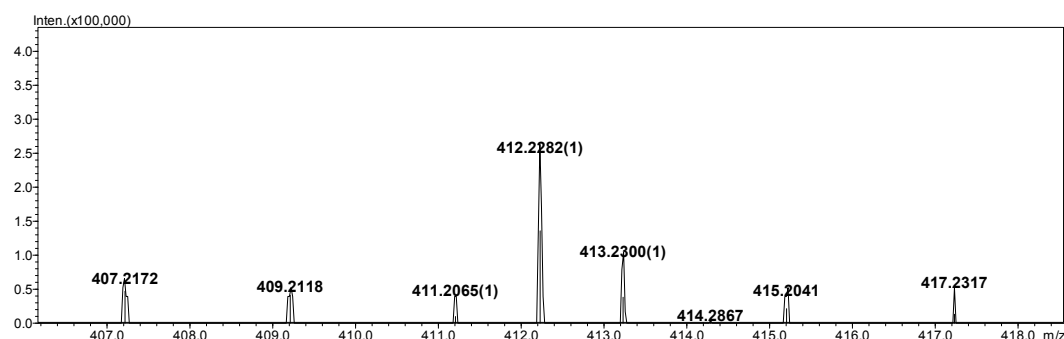


Figure S10. HRMS result of the reaction product of HXPIS with GSH.

10. Cytotoxicity experiments

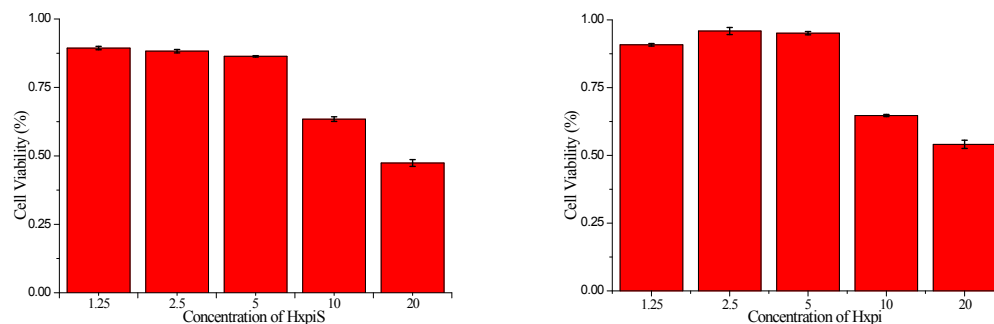
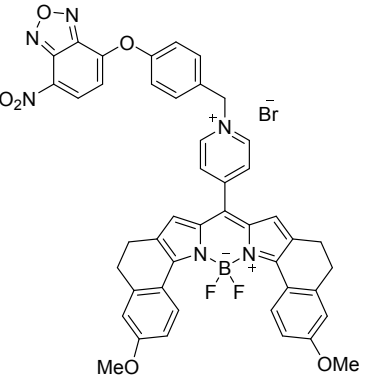
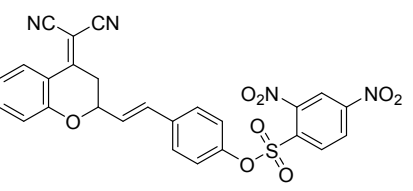
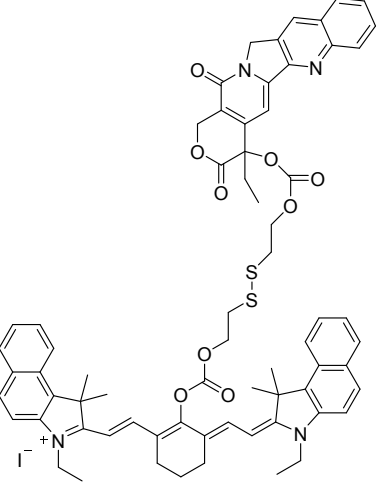
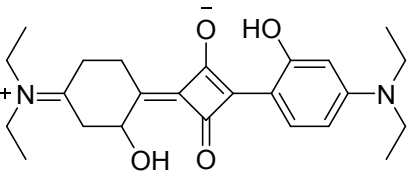
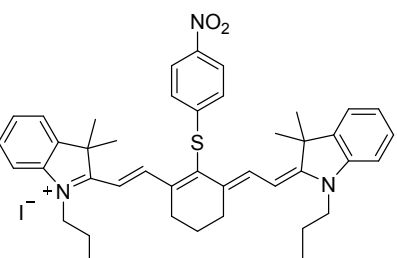


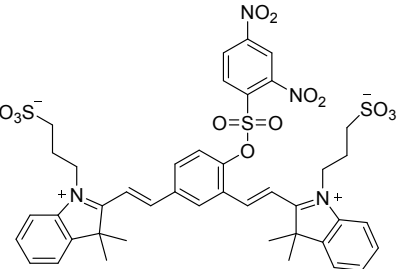
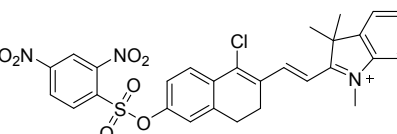
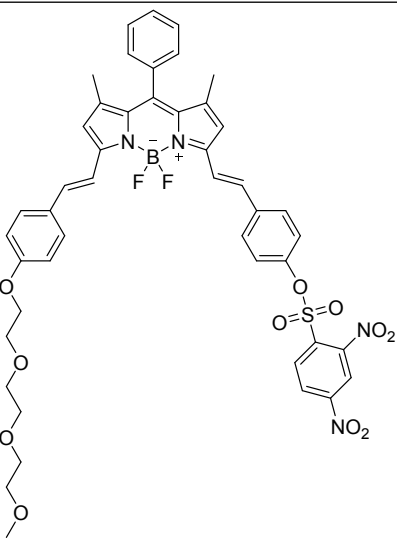
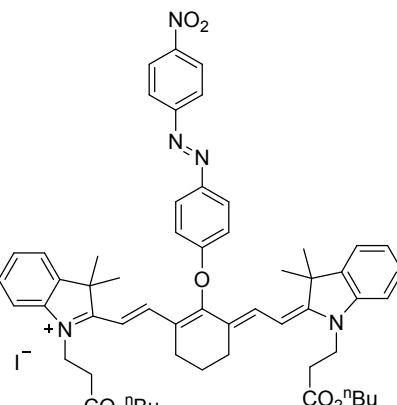
Figure S11. Cytotoxicity of different concentrations of HXPIS and HXPI to HeLa cells by a standard MTS assay, the experiment was repeated three times and the data are shown as mean (\pm S.D.).

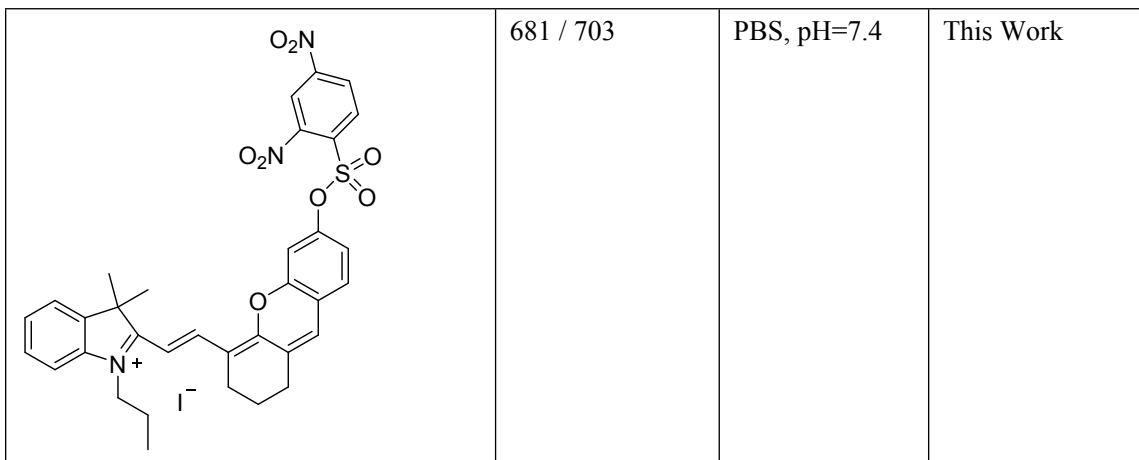
11. Table S1. Summary of the optical properties of representative near infrared fluorescent probes for distinguishing biothiols.

NIR probe	$\lambda_{\text{ex}}/\lambda_{\text{em}}$ (nm)	Solubility	References
	600/ 737	EtOH/PBS (v/v, 1: 1, pH = 7.4)	J. Mater. Chem. B, 2018, 6, 1791-1798

	600/ 746	EtOH/PBS (v/v, 3: 2, pH = 7.4).	J. Mater. Chem. B, 2018, 6, 7486-7494
	470/540 600/670	& THF/PBS (v/v, 1: 1, pH = 7.4)	Analyst, 2018, 143, 5218-5224
	646/ 661	THF/PBS (v/v, 1: 1, pH = 7.4)	Dyes and Pigments, 2018, 152, 85-92
	620/ 688	DMSO/PBS (v/v, 1: 1, pH = 7.4)	Sensor and Actuators B, 2017, 246, 988-993

	620 / 685	DMSO/PBS (v/v, 1: 1, pH = 7.4)	Sensor and Actuators B, 2018, 257, 1076-1082
	560 / 690	DMSO/H ₂ O (v/v, 1: 1, pH = 7.4)	Chem. Commun., 2014, 50, 1751-1753
	530 / 650	DMSO/PBS (v/v, 1: 1, pH = 7.4)	Chem. Sci., 2016, 7, 4958-4965
	575 / 655	CH ₃ CN/HEPES (v/v, 1: 1, pH = 9)	RSC Adv., 2015, 5, 28713-28716
	650 / 748	DMSO/HEPES (v/v, 1: 1, pH = 7.4)	RSC Adv., 2014, 4, 8360-8364

	600 / 698	PBS, pH=7.4	Org. Biomol. Chem., 2013, 11, 2098-
	550 / 680	DMSO/PBS (v/v, 1: 1, pH = 7.4)	Chem. Sci. 2016, 7, 1896-1903
	600 / 661	PBS, pH=7.4	Chem. Nano. Mat., 2016, 2, 396-399
	600 / 810	HEPES, pH=7.4	J. Am. Chem. Soc., 2014, 136, 7018-7025



12. NMR and HRMS spectra of HXPIS

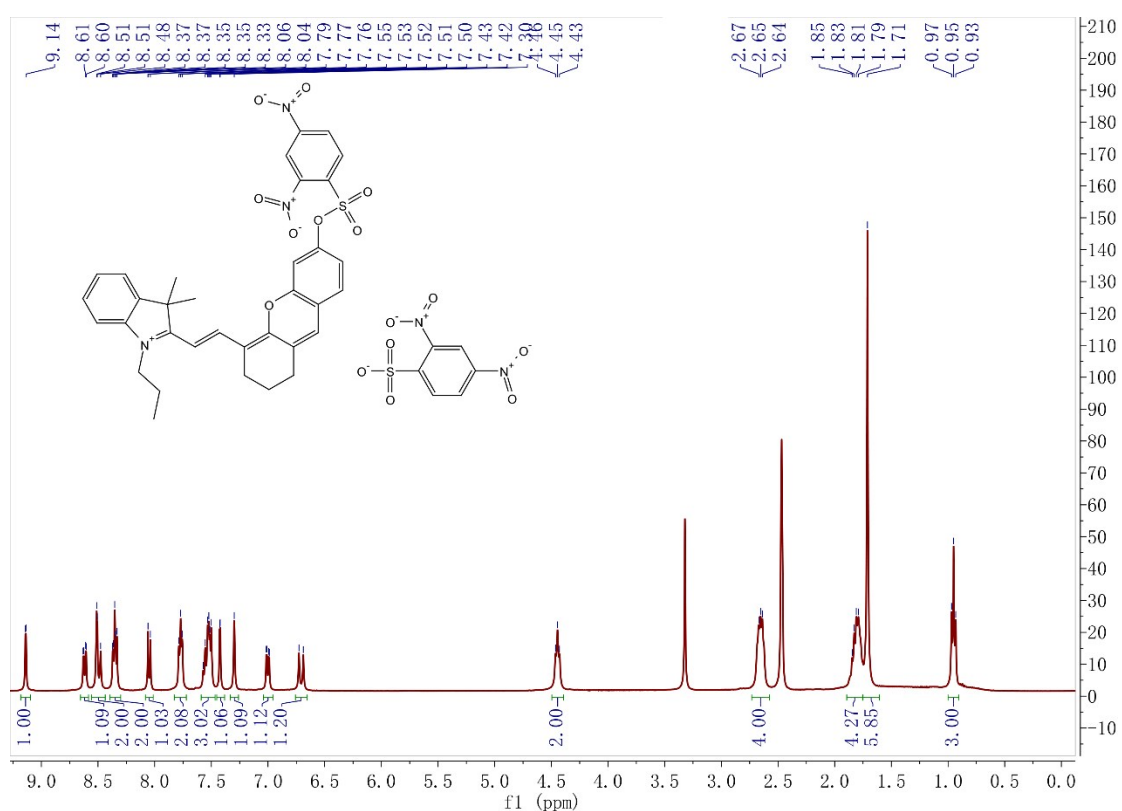


Figure S12. ^1H -NMR spectrum of HXPIS in DMSO- d_6 .

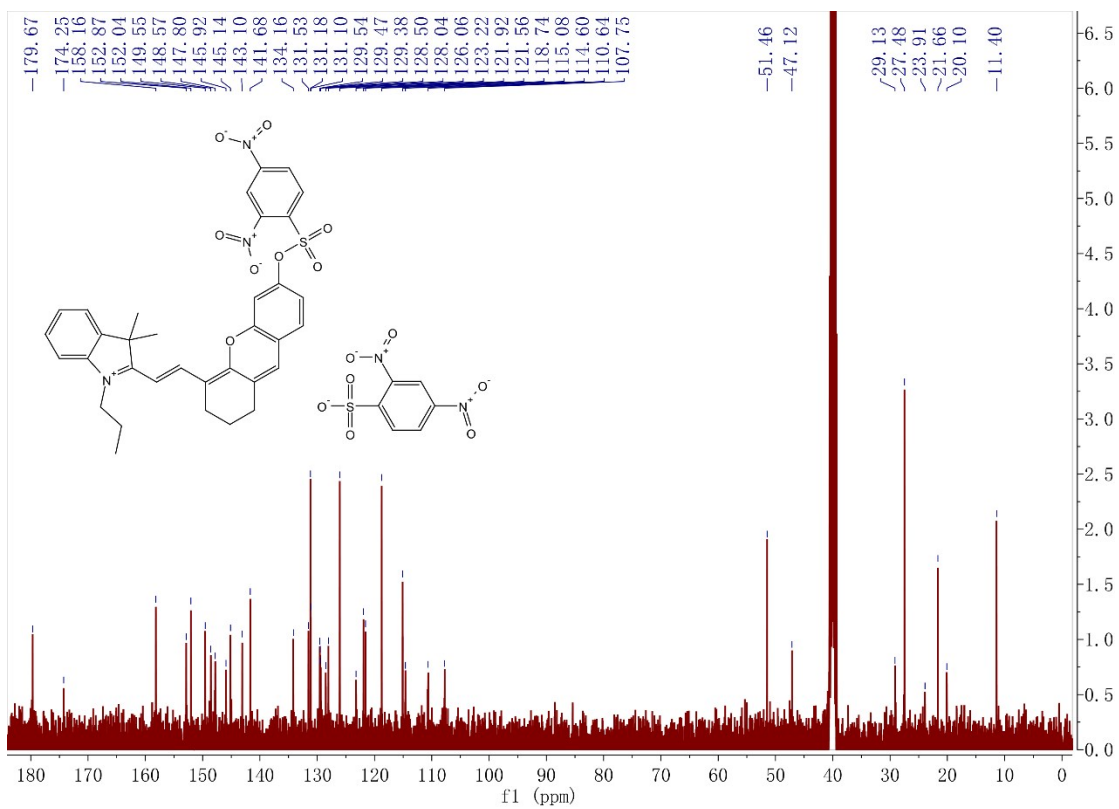


Figure S13. ^{13}C -NMR spectrum of HXPIS in DMSO-d_6 .

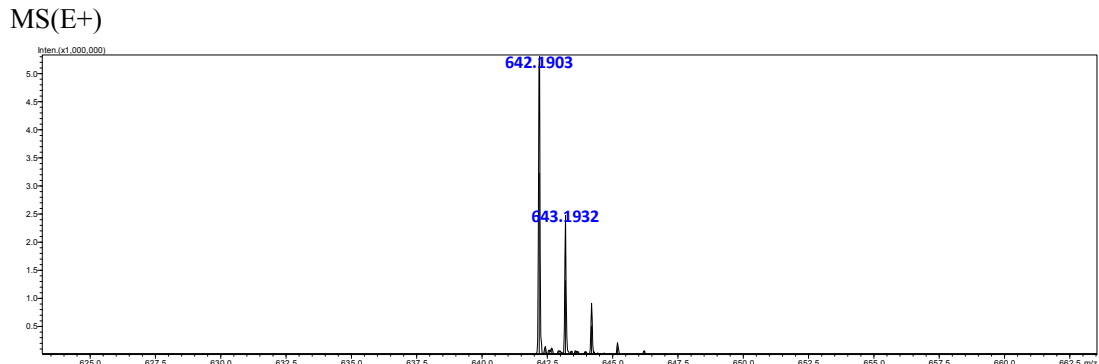


Figure S14. HRMS result of HXPIS.

Reference

- [1] L. Yuan, W.Y. Lin, S. Zhao, et al., J. Am. Chem. Soc. 134 (2012) 13510–13523.
- [2] X.F. Wu, L.H. Li, W. Shi, Q.Y. Gong, H.M. Ma, Angew. Chem. Int. Ed. 55 (2016) 14728–14732.